Parallel between the isotopic composition of coccolith calcite and carbon levels across Termination II: Developing a new paleo-CO_2 probe*

Camille Godbillot[1], Fabrice Minoletti[1], Franck Bassinot[2], Michaël Hermoso[3]

[1]Institut des Sciences de la Terre de Paris (UMR 7193 ISTeP), CNRS, Sorbonne Université, 75005 Paris, France
[2]Laboratoire des Sciences de l'Environnement et du Climat (UMR 8212 LSCE), CEA, CNRS, Université Versailles Saint Quentin, 91191, Gif sur Yvette, France
[3]Laboratoire d'Océanologie et de Géosciences (UMR 8187 LOG), Université du Littoral Côte d'Opale, CNRS, Université de Lille, 62930 Wimereux, France

Correspondence to: Camille Godbillot (camille.godbillot@sorbonne-universite.fr)

Abstract. Beyond the pCO_2 records provided by ice core measurements, the quantification of atmospheric CO_2 concentrations and changes thereof relies on proxy data, the development of which represents a foremost challenge in paleoceanography. In the paleoceanographic toolbox, the coccolithophores occupy a notable place, as the magnitude of the carbon isotopic fractionation between ambient CO_2 and a type of organic compounds that these photosynthetic microalgae synthesize (the alkenones) represents a relatively robust proxy to reconstruct past atmospheric CO_2 concentrations during the Cenozoic. The isotopic composition of coeval calcite biominerals found in the sediments and also produced by the coccolithophores (the coccoliths) have been found to record an ambient CO_2 signal through culture and sediment analyses. These studies have, however, not yet formalized a transfer function that quantitatively ties the isotopic composition of coccolith calcite to the concentrations of aqueous CO_2, and, ultimately, to atmospheric CO_2 levels. Here, we make use of a micro-separation protocol to compare the isotopic response of two size-restricted coccolith assemblages from the North Atlantic to changes in surface ocean CO_2 during Termination II (*ca.* 130-140 ka). Performing paired measurements of the isotopic composition ($\delta^{13}C$ and $\delta^{18}O$) of relatively large and small coccoliths provides an isotopic offset that can be designated as a "differential vital effect". We find that the evolution of this offset follows that of aqueous CO_2 concentrations computed from the ice core CO_2 curve and an independent temperature signal. We interpret this biogeochemical feature to be the result of converging carbon fixation strategies between large and small cells as the degree of carbon limitation for cellular growth decreases across the deglaciation. We are therefore able to outline a first-order trend between the coccolith differential vital effects and aqueous CO_2 in the range of Quaternary CO_2 concentrations. Although this study would benefit from further constraints on the other controls at play on

* We have included an alternative to this title in the point-by-point response to the comments

coccolith geochemistry (growth rate, air-sea gas exchange, etc.), this test of the drivers of coccolith $\Delta\delta^{13}C$ and $\Delta\delta^{18}O$ in natural conditions is a new step in the development of a coccolith paleo-CO_2 probe.

1 Introduction

Reconstructing the changes of atmospheric pCO_2 levels over geological timescales has been one of the major challenges in paleoenvironmental research for the last forty years (Neftel et al., 1982; Broecker, 1982; Pagani, 2013). In particular, due to its effects as a greenhouse gas, atmospheric pCO_2 is believed to have exerted a first-order control on the temperature changes at the Earth's surface that occurred over the Phanerozoic (Berner, 1990). On shorter timescales, analyses of the concentrations of CO_2 of air bubbles trapped in Quaternary ice cores, which have provided relatively direct pCO_2 estimates, have exemplified the synchronicity of pCO_2 and glacial-interglacial changes (Petit et al., 1999). Beyond 800 kyrs, however, estimates of atmospheric pCO_2 rely on more indirect proxies, mainly derived from the marine sedimentary record (Broecker, 2018). The alkenone ε_p proxy uses the magnitude of the carbon isotopic fractionation between algal lipids produced by certain haptophytes and ambient CO_2 to derive CO_2 concentrations (see review by Pagani 2013). Other proxies alternatively derive the levels of aqueous CO_2 from a set of parameters of ocean carbonate chemistry. This is the case of the foraminifera boron isotope proxy, which aims at reconstructing values for surface ocean pH (Sanyal et al., 1995; Foster, 2008) and can further be used to derive surface ocean CO_2 (Shao et al., 2019). The 45-million-year record of atmospheric pCO_2 (Zhang et al., 2013) and its 66-million-year update (Rae et al., 2021) are a flagship outcome of the ε_p and boron proxies in published literature and have yielded invaluable insights into the quantitative forcing of CO_2 decline on Earth cooling during the Cenozoic.

The coccolithophores, the same primary producers that synthesize the alkenones, also operate the intracellular biomineralization of calcite material, the coccoliths (Volkman et al., 1980). The geochemistry of these calcareous nannofossils, albeit ubiquitous in marine sediments since the Jurassic (de Vargas et al., 2007), has been overall set aside in paleoclimate reconstructions. This is due, in part, to the large biologically-induced offset between coccolith $\delta^{13}C$ and $\delta^{18}O$ compositions and that of inorganic calcite (or "vital effect") which hinders their use as traditional $\delta^{18}O$ paleo-thermometers (Dudley et al., 1986). Recent evidence has, however, shed light on the potential for the coccoliths to record past CO_2 concentrations. Numerical methods, with quantitative constraints stemming from culture data, have provided a valuable understanding on the factors dictating the magnitude of the vital effect (Rickaby et al., 2010; Bolton and Stoll, 2013; Hermoso et al., 2016a, b; McClelland et al., 2017). Collectively, these studies have shown that differences in the metabolic rates of the coccolithophores, in particular photosynthesis and calcification, can be put forward to explain the range of vital effects measured in coccolith calcite, in particular between different coccolithophore species. In turn, the rates of photosynthesis and calcification, which therefore dictate the coccolith vital effect, are dependent on the availability of CO_2 in the environment, on cell size and growth rate, on the ratio of the production of calcite relative to organic matter and on the possible expression of CO_2 concentrating mechanisms

(CCMs). As a notable corollary, the magnitude of coccolith vital effects decreases under conditions of increasing medium CO_2 (Hermoso et al., 2016b). Beyond the culture flasks of the laboratory, this result is also observed in datasets from the geological record: A global decrease in surface ocean CO_2 is believed to explain for instance why the magnitude of the vital effects of coccoliths extracted from marine sediments has increased since the late Miocene (Bolton and Stoll, 2013; Hermoso et al., 2020b). On shorter geological timescales, variations in vital effects have been observed throughout glacial-interglacial cycles (Jin et al., 2018), and tentatively linked to changes in surface ocean CO_2 (Hermoso, 2016). Using the inverse approach, attempts at deriving Eocene-Oligocene CO_2 concentrations from the vital effects of fossil coccoliths using transfer functions from culture data were successful in reproducing the pCO_2 curves obtained using the alkenone and boron paleobarometers (Tremblin et al., 2016).

Overall, data from the sedimentary record concord with results of culture experiments and numerical modelling as to the role of CO_2 on the isotopic composition of coccolith calcite for both the carbon and oxygen isotope systems. Discrepancies exist, however, between culture results, where CO_2 concentrations can be controlled, and sedimentary data. A core-top study for instance revealed that the oxygen vital effects of Noelaerhabdaceae coccoliths from sediment samples differed from close-living relatives in culture experiments (Hermoso et al., 2015). A number of methodological caveats indeed hinder the comparison of culture and sedimentary data. This includes the fact that results are obtained exclusively on monoclonal populations grown in light and nutrient-replete environments, the very little results available for coccolithophore responses in periods of low CO_2, and the short duration of culture experiments, which leaves little time for cells to adapt (Lohbeck et al., 2012).

Despite recent efforts in culture and sedimentary studies, a transfer function for the emerging coccolith vital effect-CO_2 proxy is lacking. Here, we study the isotopic response of a natural assemblage of coccoliths to changes in surface ocean CO_2 during the late Pleistocene. We isolate coccoliths of different size fractions from carbonate oozes of the mid-latitude North Atlantic core MD95-2037. We measure their specific isotopic composition, and study their departures from an inorganic reference – this offset being termed 'absolute vital effect' thereinafter. We further explore the link between the expression and magnitude of the vital effects and the hypothesized forcing of CO_2, which we derive from the atmospheric pCO_2 curves available for the interval (Bereiter et al., 2015). Specifically, we focus on Termination II (130-140 ka), during which global atmospheric pCO_2 levels increased by 80 ppm (equivalent to a 1.7 $\mu mol.kg^{-1}$ increase in $CO_{2\,aq}$). We pay specific attention to the control of environmental forcing on the isotopic composition of coccolith micro-assemblages differing in taxonomy and size, thus exploring a 'differential vital effect'. In this study, we aim to push forward the use of this differential vital effect, *i.e.* the isotopic offset between coccoliths of different sizes, as a CO_2 probe throughout the Cenozoic Era.

2 Material and Methods

2.1 Measurements of coccolith isotopic compositions

2.1.1 Ocean study site & age model

Sediment samples are from the North Atlantic core MD95-2037 (37°05'N, 32°02'W, 2630 m depth) that was retrieved during the IMAGES expedition in 1995 (Bassinot and Labeyrie, 1996). The core is located north of the Azores Current (AC), a branch of the North Atlantic Current (NAC) (**Fig. 1**). It also lies north of the Azores Front (AzF), which separates the stratified and low-productivity surface waters of the subtropical gyre in the South from the higher primary productivity region in the North where the winter mixed-layer is deeper (Lévy et al., 2005). The surface water mass is currently located in a region in relative equilibrium with respect to atmospheric CO_2 and aqueous CO_2 exchanges (**Fig. 1**). Previous studies at the site have established $\delta^{18}O$ and $\delta^{13}C$ curves for the benthic foraminifera species *Cibidoides wuellerstorfi* and the planktonic species *Globigerina bulloides* (Villanueva et al., 2001). Together with productivity records from alkenone abundances (Villanueva et al., 2001) and UK_{37}'-derived sea surface temperature (SST) records (Calvo et al., 2001), these studies have highlighted the large environmental changes that occurred in the surface ocean across Termination II in this region. This includes a 7°C increase in sea surface temperatures between the glacial maximum and full interglacial conditions, and the southward migration of the Arctic front, which, during glacial intervals, may have progressed as far South as 50°N, with implications on the stratification of the water column and the renewal of nutrients to the surface ocean (Pflaumann et al., 2003; Naafs et al., 2010; Zhang et al., 2017).

We established a new age model for site MD95-2037 over Termination II (**Fig. S1**), using the more recent reference records (such as the benthic $\delta^{18}O$ composite stacks, Lisiecki and Raymo 2005; Lisiecki and Stern 2016) developed since the last model for the site over Termination II was published (Villanueva et al., 2001). The benthic $\delta^{18}O$ signal from *Cibidoides wuellerstorfi* was first aligned to the regional benthic stack for the Deep North Atlantic by (Lisiecki and Stern, 2016) using the Analyseries software (Paillard et al., 1996). The age model was then refined by aligning the *Globigerina bulloides* $\delta^{18}O$ signal for site MD95-2037 to the stacked Corchia Cave $\delta^{18}O$ record (Tzedakis et al., 2018), as both records are expected to reflect the changes in surface temperature and ice volume that occurred across this latitudinal band (Drysdale et al., 2005). As done by Govin et al. 2015, we evaluated the accuracy of the age model by calculating the quadratic sum of the individual uncertainties deriving from i) matching errors on Analyseries; ii) the resolution of the aligned record; and iii) the dating error of the reference speleothem $\delta^{18}O$ ages. The resulting age uncertainties at our site are approximately 3 kyrs at the beginning of the interval of study during the Glacial (*ca.* 140 ka) and at the end of the interval comprising the Last Glacial Inception (*ca.* 118 ka; Calov et al. 2005). They are more modest (approx. 0.8 kyrs) during Heinrich Event 11 (H11) and the Last Interglacial (LIG).

2.1.2 Purifying coccolith fractions from core sediment samples

Sediments from the studied sections of core MD95-2037 consist of calcareous nannofossil oozes with a carbonate content ranging from 73 to 89%. Purified coccolith fractions were obtained for the interval of study (~100-145 ka) at a sampling resolution of ~20 cm at the beginning and end of the interval, and ~10 cm across Heinrich Event 11 and Termination II. We applied the separation protocol described in Minoletti et al., 2009 based on a cascade of microfiltering steps eased by gentle ultrasonic treatment. About 2g of core sediments were suspended in neutralized deionized water and sieved through a 20 μm nylon mesh to isolate the coarse fraction, while the <20 μm filtrate (fine fraction) was sequentially filtered through polycarbonate membranes of 12, 8, 5, 3 and 2 μm nominal apertures. Smear slides were prepared from the retentates of each membrane. This was done to check the granulometry and the purity of the fractions using a Zeiss Axio Imager M1 optical microscope fitted with a circular polarizer at Sorbonne Université, Paris. From the observations made on the microscope, we selected the 5-8 μm fraction where *Calcidiscus* spp. coccoliths made up 60 to 70% of the total content, and the 2-3 μm size class where *Gephyrocapsa* spp. coccoliths made up 60 to 85% of the content. These fractions were further run for isotopic analysis. Additional fine-scale observations were made using scanning electron microscopy (Zeiss Supra 55VP at Sorbonne Université) on both size fractions to check for the preservation state of the coccoliths (**Fig. S2**). For all samples, we found preservation to be good, with sparse etching and no significant overgrowth of calcite.

2.1.3 Isotopic analyses.

Between 50-80 μg of microseparated sample residues were collected for each level for both size fractions studied and introduced inside a Kiel IV Carbonate Device. The carbonate fraction was digested in ortho-phosphoric acid at 70°C, the resulting CO_2 gas was purified and run in a Delta V Advantage IRMS by Thermo Scientific for $\delta^{13}C$ and $\delta^{18}O$ analysis at Sorbonne Université. Values were calibrated relative to the Vienna Pee Dee Belemnite (‰ VPDB) via the NBS-19 international standard. Standard errors (1σ), which are calculated by running a minimum of six samples of NBS-19 per series of analyses, are ±0.05‰ for $\delta^{13}C$ and ±0.1‰ for $\delta^{18}O$ values.

2.2 Quantification of the coccolith vital effects

Coccolithophores produce their coccoliths out of isotopic equilibrium relative to the environment in which they live (Dudley et al., 1986). As our working hypothesis is that the magnitude of the vital effect in fossil coccolith calcite conveys a pCO_2 signal, it is necessary to quantify this biologically-induced isotopic phenomenon in the fossil record and to study how its magnitude evolved with a changing (CO_2) environment.

2.2.1 Absolute vital effects

Absolute vital effects are defined as the departure between the isotopic composition of the coccoliths and a theoretical inorganic calcite grown in the same conditions of temperature and isotopic composition of the medium. Previous studies have used the

foraminiferal record to derive pseudo-inorganic values for the $\delta^{13}C$ and $\delta^{18}O$ compositions of calcite (Hermoso, 2016; Jin et al., 2018; Stoll et al., 2019; Hermoso et al., 2020b), as it is possible to hand-pick individuals and apply species-specific transfer functions between foraminifera test calcite and inorganic calcite (Pearson, 2012). It must be stressed that such a biogeochemical framework heavily relies on the fact that coeval coccolithophores and planktonic foraminifera have a similar ecology (thus record the properties of the same water mass) and that foraminiferal calcite has a known and constant vital effect during the investigated time slice. Due to their relatively small vital effects and both spatially-limited and shallow living environments (Rebotim et al., 2017), foraminifera species such as *Globigerinoides ruber* and *Oribulina universa* can be regarded as adequate substrates to derive the inorganic reference. In this study, in the absence of these specific foraminifera species in the sediments, we attempt to derive the carbon isotopic composition of inorganic calcite $\delta^{13}C_{inorg}$ (in ‰ VPDB) from the composition of *Globigerina bulloides* planktonic foraminiferal calcite (Villanueva et al., 2001) using the equation in Bemis et al. 2000:

$$\delta^{13}C_{inorg} = 0.11 \times T + 2.07 + \delta^{13}C_{bulloides} \quad (Eq. 1)$$

where T is the temperature in °C and $\delta^{13}C_{bulloides}$ is expressed in ‰ VPDB. Note here that the temperature effect on the *G. bulloides* vital effect is negligible (0.71‰) over the range of temperature change (7°C) at site MD95-2037 across Termination II, when compared to the $\delta^{13}C$ fluctuations observed for the coccolith fractions (see **Results** section). The minimal 3‰ offset between *G. bulloides* and inorganic calcite $\delta^{13}C$ is among the largest measured for foraminifera species, which studies attribute to higher metabolic rates (Kahn and Williams, 1981; Bemis et al., 2000).

On the other hand, the oxygen isotope vital effect for *G. bulloides* is more restricted and is not dependent on temperature, with a reported value relative to inorganic calcite (sensu Kim and O'Neil 1997) equal to -0.52‰ (Bemis et al., 1998). We therefore calculated the inorganic reference $\delta^{18}O_{inorg}$ as follows:

$$\delta^{18}O_{inorg} = \delta^{18}O_{bulloides} + 0.52 \quad (Eq. 2)$$

with $\delta^{18}O_{inorg}$ and $\delta^{18}O_{bulloides}$ both expressed in ‰ VPDB.

From the above, we can tentatively calculate the absolute vital effects of coccoliths:

$$\Delta^{13}C_{abs} = \delta^{13}C_{coccolith} - \delta^{13}C_{inorg} \quad (Eq. 3)$$

and

$$\Delta^{18}O_{abs} = \delta^{18}O_{coccolith} - \delta^{18}O_{inorg} \quad (Eq. 4)$$

with $\delta^{13}C_{coccolith}$ and $\delta^{18}O_{coccolith}$ the isotopic compositions of either the *Gephyrocapsa*-rich 2-3 μm or the *Calcidiscus*-rich 5-8 μm fractions (in ‰ VPDB).

2.2.2 Differential vital effects.

Coccolithophore cell size exerts a major control on the expression and magnitude of vital effects in coccolithophore organic compounds (alkenones) and calcite biominerals (coccoliths) (Popp et al., 1998; Hermoso, 2014). Studies of fossil coccoliths, together with results from numerical and culture experiments (Bolton and Stoll, 2013; Hermoso et al., 2016a; McClelland et al., 2017; Hermoso et al., 2020b), have shown that the degree of utilization of carbon from the internal pool tends to become more uniform between large and small cells when carbon limitation decreases in the environment, as does their composition in $\delta^{13}C$ and $\delta^{18}O$. Under replete ambient CO_2 concentrations, the demand in carbon for the metabolism is satisfied by the supply also for the largest species, despite their smaller surface-to-volume ratio. Thus, between carbon limited- and carbon-replete conditions, the magnitude of the vital effect of a coccolith is a function of the concentration of CO_2 and of its size.

We quantify these differential vital effects (noted as the $\Delta_{\text{small-large}}$ notation) as the isotopic offsets between coccoliths differing in size, a measure directly linked to the size of the cell that produced them (Henderiks, 2008). Here, they are calculated as the difference in $\delta^{13}C$ and $\delta^{18}O$ compositions between the *Gephyrocapsa*-rich 2-3 μm and the *Calcidiscus*-rich 5-8 μm fractions.

$$\Delta^{13}\mathrm{C}_{\mathrm{small-large}} = \delta^{13}\mathrm{C}_{Gephyrocapsa-\mathrm{rich}} - \delta^{13}\mathrm{C}_{Calcidiscus-\mathrm{rich}} \quad (Eq.5)$$

and

$$\Delta^{18}\mathrm{O}_{\mathrm{small-large}} = \delta^{18}\mathrm{O}_{Gephyrocaspa-\mathrm{rich}} - \delta^{18}\mathrm{O}_{Calcidiscus-\mathrm{rich}} \quad (Eq.6)$$

with all fraction $\delta^{13}C$ and $\delta^{18}O$ expressed in ‰ VPDB.

A foremost advantage of using an isotopic offset between two "coccolith" signals is that it is not influenced by the possible biases introduced by the calculation of the isotopic composition of inorganic calcite (including temperature and the possible vital effects affecting foraminifera $\delta^{18}O$ and $\delta^{13}C$). Therefore, only the measurement of the isotopic composition of two coccolith fractions of distinct sizes is needed.

2.3 Input CO_2 values used for our calibration of the coccolith vital effects

The surface ocean is in constant chemical exchange with the atmosphere with respect to CO_2. When the air and the ocean are at equilibrium, aqueous CO_2 concentrations can be computed directly from atmospheric pCO_2 via Henry's Law, provided that sea surface temperatures (SSTs) and salinity are known (Zeebe and Wolf-Gladrow, 2001). We used the pCO_2 data from the Antarctic ice cores (Bereiter et al. 2015) to calculate equilibrium concentrations in aqueous CO_2 for site MD95-3037 over Termination II in the mixed-layer water mass, where coccolithophores thrive (Winter et al., 2002). SST estimates are taken from the alkenone-derived UK_{37}' record for the core by Calvo et al. 2001, which documents an increase from 13 to 21°C across Termination II. Salinity estimates at our site were obtained following the method of Gray and Evans 2019 by scaling the maximum salinity changes (around +1.5 psu in the glacial ocean relative to modern salinity at our site; De Vernal et al., 2005)

with the sea level curve published by Spratt and Lisiecki, 2016. Salinity varies from 34.5 during the glacial to 36 during the interglacial. Calculations of the concentration of aqueous CO_2 were made using the "seacarb" package in R (https:// CRAN.R-project.org/package=seacarb) with K_1 and K_2 constants from Lueker et al., 2000. Error estimates (1SD) for [CO_2] were obtained by running 10,000 Monte Carlo simulations with the following uncertainties: ice core pCO_2 ± 3 ppm (Petit et al., 1999), and a conservative estimate of salinity of ± 1 psu. We considered a ± 1.2°C error on SST estimates (Conte et al., 2006). The UK_{37}' paleothermometer is overall considered to yield reliable estimates of past surface sea surface temperatures (Herbert, 2003). An overestimation of UK_{37}'-derived SSTs might arise in particular when $C_{37:4}$ alkenone abundances exceed 5%, which generally occurs in locations with freshwater inputs (Calvo et al., 2002). Above this threshold, the UK_{37}'-SST relationship breaks down. Here, while $C_{37:4}$ alkenones are indeed found in larger concentrations during glacials than during interglacials at the nearby U1313 site, their concentration does not exceed 5% (Stein et al., 2009).

3. Results & Discussion

3.1 Size controls on coccolith vital effects

The relatively small coccoliths of the *Gephyrocapsa*-dominated 2-3 μm fractions exhibit $\delta^{13}C$ values that span from -0.14 to 1.70‰ **(Fig. 2)**. Larger coccoliths from the *Calcidiscus*-dominated 5-8 μm fractions exhibit more negative (=lighter) $\delta^{13}C$ compositions ranging from -1.50 to -2.36‰. This 1.5 to 3‰ difference in $\delta^{13}C$ between the isotopic compositions of the small versus the large coccoliths confirms previously observed biogeochemical data from culture experiments between *Gephyrocapsa* and *Calcidiscus* strains (Ziveri et al., 2003; Hermoso, 2014), and the observations made in sedimentological studies (Bolton and Stoll, 2013).

For the oxygen isotope system, the $\delta^{18}O$ composition of the *Gephyrocapsa* fraction ranges from 0.07 to 3.47‰, while that of the *Calcidiscus* fraction is consistently more negative across the interval, ranging from -1.01 to 1.70‰. As for the carbon system, this 1.5‰ offset is within the range of the isotopic differences between cultured *Gephyrocapsa* and *Calcidiscus* coccoliths, where the $\delta^{18}O$ of *Gephyrocapsa* coccolith calcite is typically 1 to 2‰ more positive than inorganic calcite, and 2 to 3‰ more positive than *Calcidiscus* coccolith calcite (Ziveri et al., 2003; Candelier et al., 2013; Hermoso et al., 2016a).

Culture and numerical experiments have attributed the large isotopic difference in both carbon and oxygen systems between *Gephyrocapsa* and *Calcidiscus* coccoliths to the different strategies of carbon acquisition between coccolithophore cells of different sizes. In the carbon system on the one hand, small cells are less sensitive to limitations in the diffusive supply of CO_2 to the cell due to a relatively larger surface-to-volume ratio than larger cells (Popp et al., 1998; Burkhardt et al., 1999). This enables small cells to fix more carbon through photosynthesis, and in turn, they produce coccoliths from a remaining internal carbon pool with a more positive ("heavier") $\delta^{13}C$ composition than larger cells (McClelland et al., 2017). On the other hand,

the factors driving the array of oxygen vital effects amongst strains are not so well constrained. There is compelling evidence that coccoliths are isotopically mineralized from HCO_3^- ions that are pumped from the intracellular carbon pool into the coccolith vesicle (Nimer et al., 1994; Brownlee and Taylor, 2004). It has been hypothesized that the degree of equilibration between CO_2 and water molecules inside the intracellular carbon pool sets the amplitude of the coccoliths' vital effect (Hermoso et al., 2016a). Hence small cells, which calcify more quickly than large cells, source HCO_3^- that has maintained the original "heavy" $\delta^{18}O$ composition of the CO_2 diffused through the cell membrane, and ultimately produce coccoliths with a more positive $\delta^{18}O$ than large cells.

Overall, coccolith $\delta^{13}C$ and $\delta^{18}O$ across Termination II confirm the size-dependence of isotopic signals observed in culture and numerical experiments. In this next part, we will try and establish how these isotopic compositions compare to the inorganic reference computed from the isotopic composition of foraminiferal tests in the sedimentary record, since, in culture and numerical experiments, the magnitude of coccolith vital effects has been tied to the degree of carbon limitation in the medium (Rickaby et al., 2010; Hermoso, 2014; Hermoso et al., 2020a).

3.2 Controls on absolute coccolith vital effects

As shown in **Fig. 3**, both coccolith size fractions exhibit very negative $\delta^{13}C$ compositions relative to the computed values for inorganic calcite. The small 2-3 μm coccolith fraction lies 1 to 3‰ below inorganic calcite, while the offset is around -5‰ for the larger 5-8 μm fraction (**Fig. 3**). This offset is reduced in the oxygen system: The 2-3 μm fraction has a $\delta^{18}O$ composition close to that of inorganic calcite (an approximate +0.2‰ offset), while the 5-8 μm fraction exhibits a mean +1.3‰ offset relative to inorganic calcite (**Fig. 3**).

Taking the foraminifera-derived inorganic reference at face value, it thus appears that the magnitude of $\Delta^{13}C_{abs}$ for both size fractions is much larger than those observed for cultured coccoliths. In culture experiments, *Gephyrocapsa* typically displays an absolute vital effect in carbon and oxygen between -1 and 0‰ and between 1.0 and 1.3‰, respectively. *Calcidiscus* coccolith calcite typically lies 0.5 to 2‰ below inorganic calcite in both carbon and oxygen systems (Hermoso, 2014; Hermoso et al., 2016b; McClelland et al., 2017). We suggest that these differences result from the calculation of the inorganic reference from foraminifera isotopic records. Most empirical equations from culture experiments linking the isotopic composition of foraminifera tests to that of inorganic calcite are tested under changing medium temperature (Bemis et al., 2000, 1998). In the present study specifically, the use of the isotopic composition of *Globigerina bulloides* to estimate the $\delta^{13}C$ and $\delta^{18}O$ of inorganic calcite is additionally hindered by the large uncertainties surrounding this foraminifera's vital effect and its life cycle within the water column. *G. bulloides* indeed has one of the largest vital effects among foraminifera: The isotopic composition of its test lies respectively 4‰ and 0.5‰ below that of inorganic calcite in the carbon and oxygen systems in the surface ocean (Kahn and Williams, 1981), an array of values consistent with results from culture experiments (Bemis et al., 1998, 2000) (**Fig. 3**). The -4‰ offset in the carbon system is however reduced to 2‰ at a 100 m depth where this species thrives (Kahn

and Williams, 1981). Similarly, the offset in the oxygen system varies from 0.5‰ to 1.5‰ in the first 100 m (Kahn and Williams, 1981). As large uncertainties persist as to the calcification depth of this foraminifera, which migrates down the water column during its life cycle (Blanc and Bé, 1981), we are unable to derive a reliable and accurate measurement of the isotopic composition of inorganic calcite from *G. bulloides*. Thus overall, we deem the uncertainties surrounding the computation of coccolith vital effects too large to interpret their changes across the interval.

3.3 Controls on differential coccolith vital effects

Having highlighted the different biases affecting the interpretation of absolute vital effect results in this study, we choose to focus the rest of our interpretations on the differential vital effects, which do not require the computation of an inorganic reference. Several studies in the geological record (Bolton and Stoll, 2013; Tremblin et al., 2016; Hermoso et al., 2020b) indeed suggest their variations carry an environmental signal, which we propose to test and quantify below.

3.3.1 Covariation of differential vital effects across the interval of study

In this study, coccoliths from the *Gephyrocapsa* 2-3 µm fraction exhibit more positive vital effects for both carbon and oxygen than the larger coccoliths throughout the interval (a mean of 2.8‰ and 1.5‰, respectively; **Fig. 3**). This, as detailed above, is within the range of the vital effect differences observed in culture experiments between *Gephyrocapsa* and *Calcidiscus* strains. Interestingly, the isotopic offset between both size fractions is not constant through time. In detail, the largest offset for both carbon and oxygen vital effects is found at the beginning of the interval in the glacial ocean (at 3.81 and 2.38‰ respectively). Both $\Delta^{13}C_{small\text{-}large}$ and $\Delta^{18}O_{small\text{-}large}$ generally decrease across the deglaciation. They reach a minimum during the cold Heinrich Event 11 (1.57 and 0.68‰, respectively). Relatively steady during the Last Interglacial, the $\Delta^{13}C_{small\text{-}large}$ and $\Delta^{18}O_{small\text{-}large}$ increase at the onset of the last glaciation. Over the entire interval, $\Delta^{13}C_{small\text{-}large}$ and $\Delta^{18}O_{small\text{-}large}$ display a regression coefficient (r^2) of 0.80 and a *p*-value < 10^{-7}: When the difference in $\delta^{13}C$ between small and large coccolith size fractions increases, the offset in their $\delta^{18}O$ increases as well. Similar results were obtained by Bolton and Stoll 2013; Hermoso et al. 2020 in the fossil record in two case studies spanning intervals of the Miocene. They argue that an environmental parameter, namely CO_2, is at the origin of the variations of both carbon and oxygen differential vital effects.

3.3.2 Controls of CO_2 on carbon and oxygen differential vital effects

Coccolithophores rely on available aqueous CO_2 in the surface ocean to fix carbon both through photosynthesis and calcification (Hein and Sand-Jensen, 1997; Monteiro et al., 2016). The $\Delta^{13}C_{small\text{-}large}$ and $\Delta^{18}O_{small\text{-}large}$ offsets show a statistically significant correlation with changes in the ambient CO_2 concentrations (r^2 =0.44, $p < 10^{-2}$ and $r^2 = 0.51$, $p < 10^{-3}$, respectively; **Fig. 4**). When the CO_2 content increases in the surface ocean, the isotopic offset between large and small coccoliths decreases. The relationship with atmospheric pCO_2 as recorded in the Antarctic ice cores is not as significant, however, with a r^2 of 0.27 ($p = 0.02$) between coccolith $\Delta^{13}C_{small\text{-}large}$ and ice core pCO_2, and a r^2 of 0.37 ($p < 0.01$) with $\Delta^{18}O_{small\text{-}large}$ (**Fig. S3**). The largest decoupling between atmospheric and oceanic CO_2 over the interval occurs during Heinrich Event 11. This marked cold event

in the mid-latitude North Atlantic (Jiménez-Amat and Zahn, 2015; Deaney et al., 2017) leads to a short-lived event of increased pCO_2 solubility and thus increased aqueous CO_2 concentrations (*ca.* 9 μmol.kg^{-1}). This peak in oceanic CO_2 levels, which does not appear in the global atmospheric pCO_2 record, coincides with the lowest magnitudes of differential coccolith vital effects across the interval.

Culture and numerical studies offer insight into the way that changes in CO_2 concentrations drive the variations in the difference in $\delta^{13}C$ and $\delta^{18}O$ of small versus large cells (Bolton and Stoll, 2013; Hermoso et al., 2016b; McClelland et al., 2017). In the modern ocean, phytoplankton cells experience CO_2 limitation (Hein and Sand-Jensen, 1997; Reinfelder, 2011). This is especially the case for the larger cells, which are less permeable to ambient CO_2 due to a small surface-to-volume ratio (Popp et al., 1998). Culture studies have demonstrated that when CO_2 concentrations in the culture medium increase, increasing photosynthetic carbon fixation in large cells drives their coccolith $\delta^{13}C$ towards "heavier" values, thereby reducing the $\Delta^{13}C_{small\text{-}large}$ (Hermoso et al., 2016b; McClelland et al., 2017). In the oxygen system, the reduction of $\Delta^{18}O_{small\text{-}large}$ under conditions of increasing CO_2 is explained by an increase in the equilibration time of HCO_3^- with CO_2 in small cells, due to a larger supply of CO_2 from the environment into the intracellular pool. As a result, their coccolith $\delta^{18}O$ evolves towards "lighter" values, similar to that of large coccoliths.

In agreement with culture results, both $\Delta^{13}C_{small\text{-}large}$ and $\Delta^{18}O_{small\text{-}large}$ scale inversely with CO_2 changes over the interval. A standard OLS regression models yields the following relationship between coccolith differential vital effects and aqueous CO_2 for aqueous CO_2 concentrations below 10 μmol.kg^{-1} (Eqs. 7 and 8, for the carbon and oxygen isotopic systems, respectively):

$$CO_2\ (\pm 0.51) = -0.76 \times \Delta^{13}C_{small-large} + 10.47 \qquad (Eq.7)$$

$$CO_2\ (\pm 0.48) = -1.15 \times \Delta^{18}O_{small-large} + 10.04 \qquad (Eq.8)$$

with CO_2 in μmol.kg^{-1}, and $\Delta^{13}C_{small\text{-}large}$ and $\Delta^{18}O_{small\text{-}large}$ in ‰ VPDB. Compared to the CO_2 ranges tested in culture experiments (typically 1 to 5 times present-day concentrations; Rickaby et al., 2010; Bach et al., 2013; Hermoso et al., 2016b), the range of the increase in surface ocean aqueous CO_2 at site MD95-2037 corresponding to the atmospheric pCO_2 change throughout Termination II is arguably small in absolute values (1.9 μmol.kg^{-1} at core MD95-2037). However, the rise from 7.3 to 9.2 μmol.kg^{-1} represents a 25% relative increase in CO_2 over the deglaciation in a very carbon-limited ocean, and is thus likely to trigger a strong response in coccolith metabolic rates. This is evident in **Fig. 5**, which shows that the sensitivity of coccolith differential vital effects to the measured changes in CO_2 in our study is twice as large as the one derived from the datasets of Bolton et al., 2012 for the Late Miocene on similar coccolith size fractions (see **Table S1** for details on the datasets used).

The largest change in carbon and oxygen differential vital effects occurs at the end of MIS 6, from the onset to the peak of Heinrich Event 11 centred around 132 ka. In the glacial (G) ocean, during the Last Interglacial (LIG) and the Glacial Inception (GI), differential vital effects display a variability that does not seem to correspond to a change in CO_2 levels (**Fig. 4**). This might be due to either i) processes other than CO_2 affecting coccolithophore calcification and photosynthesis and thus vital effects (*i.e.* growth rate, carbon concentrating mechanisms) or ii) a disequilibrium between atmosphere and seawater CO_2 concentrations. These points are discussed below.

3.3.3 Impact of coccolithophore physiology changes on differential vital effects

The direct comparison of coccolith differential vital effects to CO_2 concentrations can be complicated by the influence of a number of physiological factors affecting the geochemistry of the coccolithophores. In addition to the cellular surface-to-volume ratio and supply of carbon in the form of CO_2 already mentioned above, coccolith vital effects are also dependent on growth rate (μ), and the possible presence of CO_2 concentrating mechanisms (CCMs).

At a given [CO_2], larger division rates increase the demand of the cell for carbon (Popp et al., 1998). Larger division rates might therefore increase coccolith vital effects in the absence of any change of [CO_2]. However, modeling and culture results reveal an inverse relationship linking cell size (thus surface/volume ratio) and growth rate (Huete-Ortega et al., 2012; Aloisi, 2015), which suggests that any change in growth rate is theoretically compensated by a change in cell size. If across the interval there is nevertheless a shift towards coccolithophore assemblages with larger growth rates within a given size fraction, this could reduce the efficiency of coccolithophore photosynthesis and calcification. Specifically, an increase in growth rate with no observable change in cell size could explain why $\Delta^{13}C_{small\text{-}large}$ and $\Delta^{18}O_{small\text{-}large}$ increase between the LIG and GI despite similar [CO_2] (**Fig. 5**). The alkenone concentrations available at this site over Termination II (Villanueva et al., 2001), a proxy for growth rate changes, indeed report that coccolithophore productivity varied over the interval. However, they are uncorrelated to coccolithophore differential vital effects (**Fig. S3**). Including alkenone concentrations in Eqs. 7 and 8 relating coccolith differential vital effects to aqueous CO_2 does not lead to better regression coefficients. Overall, this suggests that growth rate changes are not responsible for the observed discrepancies between $\Delta^{13}C_{small\text{-}large}$, $\Delta^{18}O_{small\text{-}large}$ and [CO_2].

In addition to growth rate changes, the presence of CO_2 concentrating mechanisms (CCMs) can also affect the sensitivity of the vital effect to changing CO_2 concentrations. These mechanisms, which might include the excretion of carbonic anhydrase (CA) or dissolved inorganic carbon transporters (Reinfelder, 2011), increase the carbon supply, either from the environment to the cell, or from the cytoplasm to the chloroplast. Over our interval of study, the presence of CCMs in coccolithophores of both coccolith size fractions might explain why some $\Delta^{13}C_{small\text{-}large}$ and $\Delta^{18}O_{small\text{-}large}$ values of the glacial maximum are low, despite low ambient CO_2. Previous studies have invoked the presence of CCMs to explain why the transfer function established for the alkenone ε_p-barometer is not suitable for periods with low surface ocean CO_2 levels such as glacial maxima (Stoll et al., 2019; Badger et al., 2019). Here, only a fraction of the $\Delta^{13}C_{small\text{-}large}$ and $\Delta^{18}O_{small\text{-}large}$ data points in the low-CO_2 surface

ocean lie aside the general trend, indicating no threshold value below which coccolithophore inducible CCMs might be upregulated. This is compatible with observations from culture experiments performed on *Emiliania huxleyi* that report that CCMs are upregulated in the cell when $[CO_2]$ falls below 7.5 $\mu mol.kg^{-1}$ in the medium (Bach et al., 2013). It is also compatible with results from other culture experiments which find no CCM upregulation in *Gephyrocapsa* cells in conditions of carbon limitation (Nimer et al., 1997). Moreover, under the standing hypothesis, CCM upregulation must impact both photosynthesis and calcification rates in order to explain why glacial values for both $\Delta^{13}C_{small\text{-}large}$ and $\Delta^{18}O_{small\text{-}large}$ lie off the general trend, respectively. However, previous gene sequencing and modelling studies suggest that cellular CCM upregulation acts predominantly at the chloroplast level to boost photosynthesis, with little effect on calcification (Bach et al., 2013). On the whole, we deem the presence of CCMs to be unlikely across the interval.

3.4 Impact of air-sea gas exchange on $[CO_2]$ calculations

The surface ocean CO_2 values calculated from the ice core atmospheric pCO_2 records and alkenone UK_{37}' cover two discrete ranges of carbon levels that do not overlap: A "glacial" CO_2 range centered around 7.5 $\mu mol.kg^{-1}$ and an "interglacial" CO_2 range centered around 9 $\mu mol.kg^{-1}$ (**Fig. 5**). Coccolith differential vital effects, on the other hand, paint a more nuanced picture over the interval, with no notable gap in values over the interval in either $\Delta^{13}C_{small\text{-}large}$ or $\Delta^{18}O_{small\text{-}large}$. Having exposed in the previous section the different uncertainties affecting coccolith differential vital effects, we review below the potential biases likely to affect the reconstruction of the $[CO_2]$ figures, and therefore the input values of our calibration.

The largest uncertainty when deriving surface ocean CO_2 values from atmospheric CO_2 arises from the chemical disequilibrium existing at the air-sea interface. In the modern ocean, surface ocean CO_2 concentrations might lie as high as 100 ppm yearly above atmospheric pCO_2 in equatorial regions or as low as -50 ppm in the Arctic (Takahashi et al., 2011). The range of air-sea disequilibrium is more restricted in the mid-latitude North Atlantic. To the north of the Azores Front, the existence of a deep winter mixed layer enables the cycling of nutrient at the surface and promotes primary productivity, leading surface CO_2 to be slightly lower than atmospheric CO_2. This disequilibrium promotes the dissolution of atmospheric CO_2 in the surface ocean, creating a 15 ppm yearly sink for global pCO_2 at site MD95-2037. Coccolith-derived $[CO_2]$ would indicate a value of ~ 0.8 $\mu mol.kg^{-1}$ (around 20 ppm) below those computed from ice core pCO_2 records during the glacial inception. This is equivalent to the disequilibrium at the site in today's "glacial inception" surface ocean. However, the existence of the 15 ppm sink cannot account for the coccolith-derived $[CO_2]$ values of the glacial maximum. Instead, when taking coccolith $[CO_2]$ at face value, surface ocean conditions exceed ice core pCO_2 by 20 ppm in the glacial ocean.

There is compelling evidence that air-sea pCO_2 disequilibrium (ΔpCO_2) varied in the past (Skinner et al., 2010; Martínez-Botí et al., 2015; Skinner et al., 2017). Data from boron isotopes, for instance, reveal that a widespread outgassing event, produced by the renewed upwelling of carbon-rich deep waters, enriched the surface ocean by as much as 60 ppm relative to the

atmosphere over the last deglaciation (Shao et al., 2019). The existence of a high surface ocean CO_2 event at the onset of deglaciations had previously been hypothesized and put forward to explain the higher than expected ε_p measured during glacial maxima (Jasper et al., 1994). While the composite ΔpCO_2 plot obtained by Shao et al. 2019 cannot account for regional disparities, the existence of an outgassing event could explain the 20 ppm excess of glacial coccolith-derived CO_2 relative to the Antarctic record. An alternative hypothesis might include a weakening of the soft-tissue pump relative to the carbonate counter pump during the glacial maximum (Duchamp-Alphonse et al., 2018), leading to the formation of an oceanic pCO_2 source to the atmosphere. This could result from a stronger stratification of the water column during glacial maxima caused by the expansion of polar (melt)waters as low as 50°N (Villanueva et al., 1998; Pflaumann et al., 2003). The poor renewal of surface ocean nutrient concentration during the glacial maximum (Skinner et al., 2010), together with low glacial SSTs, may have weakened the biological pump. At the same time, both modelling and sedimentological results suggest that coccolithophore calcification spiked during glacial maxima in the midlatitude North Atlantic (Beaufort et al., 2011; Omta et al., 2013). This may have strengthened the carbonate counter pump, and made the mid-latitude North Atlantic glacial ocean a weak source for atmospheric carbon immediately before the deglaciation.

A change in the value of air-sea disequilibrium over the deglaciation can thus provide a likely explanation for the discrepancies between the ice core pCO_2 and coccolith vital effect records across the deglaciation. This bias is common to the different pCO_2 proxies calibrated using ice core data, because the extent of the change in the disequilibrium, which remains difficult to quantify, can, in all likelihood, represent up to half of the atmospheric pCO_2 changes across a deglaciation.

4 Conclusions

The paleobiogeochemical records presented in this study throw light on the nature of the factors forcing both the isotopic composition of the coccoliths and the magnitude of the vital effects in relatively small versus large coccoliths. We take advantage of the major and well constrained pCO_2 rise that occurs over the penultimate deglaciation between 140 and 130 kyrs to study the response of the differential coccolith vital effects to ambient CO_2 levels. We validate results from previous culture and numerical experiments, in that the difference between the isotopic composition between small and large coccolith size fractions responds to a forcing exerted by the availability of CO_2, which sustains both cellular photosynthesis and calcification. This study outlines the "low CO_2" endmember of a more general transfer function tying the differential coccolith vital effects ($\Delta^{13}C_{small\text{-}large}$ and $\Delta^{18}O_{small\text{-}large}$) to an ambient CO_2 concentration, applicable to periods such as Pleistocene glacial-interglacial cycles. However, a more detailed record of the oceanographic and primary productivity changes that occur over the deglaciation is needed before this relationship can be defined beyond a first order trend. This works sets the foundations for the use of coccolith differential vital effects to extend the ice core pCO_2 records into Quaternary time periods of particular interest. This includes target intervals such as the Mid-Pleistocene Transition (*ca.* 1250-700 ka), over which no ice-derived

CO_2 record currently exists, and during which variations in atmospheric pCO_2 concentrations are believed to have caused the changes of the glacial-interglacial pace from 40 to 100-kyr-cyclicity.

Data availability

The data used will be available from the Pangaea data repository upon acceptance of the publication.

Author contributions

M.H. and F.M. designed research; C.G. prepared samples; C.G., F.M., F.B. and M.H. analyzed data; and C.G. wrote the paper with inputs from F.M., F.B. and M.H.

Competing interests

The authors declare that they have no conflict of interest.

Acknowledgements

We thank Nathalie Labourdette, Lorna Foliot, Laura Lutaster and Laurent Emmanuel for measurements of the isotopic ratios of carbonates, and Omar Boudouma for help on the SEM. This study benefited from insightful discussions with Jérémie Bardin. We would also like to thank Eva Calvo and Clara Bolton who gave us access to their data. Finally, we are grateful to the Editor Luc Beaufort, Tom Dunkley Jones and an anonymous reviewer for their constructive comments, which greatly improved the manuscript.

Financial support

M.H. acknowledges financial support from the French *Agence Nationale de la Recherche* (ANR) – Project "CARCLIM" under reference ANR-17-CE01-0004-01. Part of this work was also supported by the *Mission pour l'Interdisciplinarité* of the French *Centre National de la Recherche Scientifique* (CNRS) in the framework of the *Défi ISOTOP* with a grant awarded to Fabrice Minoletti – Project "COCCOTOP".

References

Aloisi, G.: Covariation of metabolic rates and cell size in coccolithophores, Biogeosciences, 12, 4665–4692, https://doi.org/10.5194/bg-12-4665-2015, 2015.

Bach, L. T., MacKinder, L. C. M., Schulz, K. G., Wheeler, G., Schroeder, D. C., Brownlee, C., and Riebesell, U.: Dissecting the impact of CO2and pH on the mechanisms of photosynthesis and calcification in the coccolithophore Emiliania huxleyi, New Phytol., 199, 121–134, https://doi.org/10.1111/nph.12225, 2013.

Badger, M. P. S., Chalk, T. B., Foster, G. L., Bown, P. R., Gibbs, S. J., Sexton, P. F., Schmidt, D. N., Pälike, H., Mackensen, A., and Pancost, R. D.: Insensitivity of alkenone carbon isotopes to atmospheric CO2 at low to moderate CO2 levels, Clim. Past, 15, 539–554, https://doi.org/10.5194/cp-15-539-2019, 2019.

Bassinot, F. and Labeyrie, L.: IMAGES - MD 101 à bord du Marion-Dufresne du 29 mai au 11 juillet 1995. A coring cruise of the R/V Marion Dufresne in the North Atlantic Ocean and Norwegian Sea., Les Publ. l'Institut français pour la Rech. la Technol. polaires. Les Rapp. des campagnes à la mer, 96–1, 221p, 1996.

Beaufort, L., Probert, I., De Garidel-Thoron, T., Bendif, E. M., Ruiz-Pino, D., Metzl, N., Goyet, C., Buchet, N., Coupel, P., Grelaud, M., Rost, B., Rickaby, R. E. M., and De Vargas, C.: Sensitivity of coccolithophores to carbonate chemistry and ocean acidification, Nature, 476, 80–83, https://doi.org/10.1038/nature10295, 2011.

Bemis, B. E., Spero, H. J., Bijma, J., and Lea, D. W.: Reevaluation of the oxygen isotopic composition of planktonic foraminifera: Experimental results and revised paleotemperature equations, Paleoceanography, 13, 150–160, https://doi.org/10.1029/98PA00070, 1998.

Bemis, B. E., Spero, H. J., Lea, D. W., and Bijma, J.: Temperature influence on the carbon isotopic composition of Globigerina bulloides and Orbulina universa (planktonic foraminifera), Mar. Micropaleontol., 38, 213–228, https://doi.org/10.1016/S0377-8398(00)00006-2, 2000.

Bereiter, B., Eggleston, S., Schmitt, J., Nehrbass-Ahles, C., Stocker, T. F., Fischer, H., Kipfstuhl, S., and Chappellaz, J.: Revision of the EPICA Dome C CO2 record from 800 to 600 kyr before present, Geophys. Res. Lett., 42, 542–549, https://doi.org/10.1002/2014GL061957, 2015.

Berner, R. A.: Atmospheric Carbon Dioxide Levels Over Phanerozoic Time, Science (80-.)., 249, 1382–1386, https://doi.org/10.1126/science.249.4975.1382, 1990.

Blanc, P.-L. and Bé, A. W. H.: Oxygen-18 Enrichment of Planktonic Foraminifera Due to Gametogenic Calcification Below the Euphotic Zone, Science (80-.)., 213, 1247–1250, https://doi.org/10.1126/science.213.4513.1247, 1981.

Bolton, C. T. and Stoll, H. M.: Late Miocene threshold response of marine algae to carbon dioxide limitation, Nature, 500, 558–562, https://doi.org/10.1038/nature12448, 2013.

Bolton, C. T., Stoll, H. M., and Mendez-Vicente, A.: Vital effects in coccolith calcite: Cenozoic climate- pCO2 drove the diversity of carbon acquisition strategies in coccolithophores?, Paleoceanography, 27, 1–16, https://doi.org/10.1029/2012PA002339, 2012.

Broecker, W.: CO2: Earth's Climate Driver, Geochemical Perspect., 7, 117–196, https://doi.org/10.7185/geochempersp.7.2, 2018.

Broecker, W. S.: Glacial to interglacial changes in ocean chemistry, Prog. Oceanogr., 11, 151–197, https://doi.org/10.1016/0079-6611(82)90007-6, 1982.

Brownlee, C. and Taylor, A.: Calcification in coccolithophores: A cellular perspective, 31–49, https://doi.org/10.1007/978-3-662-06278-4_2, 2004.

Burkhardt, S., Riebesell, U., and Zondervan, I.: Effects of growth rate, CO2 concentration, and cell size on the stable carbon isotope fractionation in marine phytoplankton, Geochim. Cosmochim. Acta, 63, 3729–3741, https://doi.org/10.1016/S0016-7037(99)00217-3, 1999.

Calov, R., Ganopolski, A., Claussen, M., Petoukhov, V., and Greve, R.: Transient simulation of the last glacial inception. Part I: Glacial inception as a bifurcation in the climate system, Clim. Dyn., 24, 545–561, https://doi.org/10.1007/s00382-005-0007-6, 2005.

Calvo, E., Villanueva, J., Grimalt, J. O., Boelaert, A., and Labeyrie, L.: New insights into the glacial latitudinal temperature gradients in the North Atlantic. Results from U37K′ sea surface temperatures and terrigenous inputs, Earth Planet. Sci. Lett., 188, 509–519, https://doi.org/10.1016/S0012-821X(01)00316-8, 2001.

Calvo, E., Grimalt, J., and Jansen, E.: High resolution U37K sea surface temperature reconstruction in the Norwegian Sea during the Holocene, Quat. Sci. Rev., 21, 1385–1394, https://doi.org/10.1016/S0277-3791(01)00096-8, 2002.

Candelier, Y., Minoletti, F., Probert, I., and Hermoso, M.: Temperature dependence of oxygen isotope fractionation in coccolith calcite: A culture and core top calibration of the genus Calcidiscus, Geochim. Cosmochim. Acta, 100, 264–281, https://doi.org/10.1016/j.gca.2012.09.040, 2013.

Conte, M. H., Sicre, M. A., Rühlemann, C., Weber, J. C., Schulte, S., Schulz-Bull, D., and Blanz, T.: Global temperature calibration of the alkenone unsaturation index (U 37k) in surface waters and comparison with surface sediments, Geochemistry, Geophys. Geosystems, 7, https://doi.org/10.1029/2005GC001054, 2006.

Deaney, E. L., Barker, S., and Van De Flierdt, T.: Timing and nature of AMOC recovery across Termination 2 and magnitude of deglacial CO2 change, Nat. Commun., 8, https://doi.org/10.1038/ncomms14595, 2017.

Drysdale, R. N., Zanchetta, G., Hellstrom, J. C., Fallick, A. E., and Zhao, J. X.: Stalagmite evidence for the onset of the Last Interglacial in southern Europe at 129 ± 1 ka, Geophys. Res. Lett., 32, 1–4, https://doi.org/10.1029/2005GL024658, 2005.

Duchamp-Alphonse, S., Siani, G., Michel, E., Beaufort, L., Gally, Y., and Jaccard, S. L.: Enhanced ocean-atmosphere carbon partitioning via the carbonate counter pump during the last deglacial, Nat. Commun., 9, 2396, https://doi.org/10.1038/s41467-018-04625-7, 2018.

Dudley, W. C., Blackwelder, P., Brand, L., and Duplessy, J. C.: Stable isotopic composition of coccoliths, Mar. Micropaleontol., 10, 1–8, https://doi.org/10.1016/0377-8398(86)90021-6, 1986.

Foster, G. L.: Seawater pH, pCO2 and [CO2-3] variations in the Caribbean Sea over the last 130 kyr: A boron isotope and B/Ca study of planktic foraminifera, Earth Planet. Sci. Lett., 271, 254–266, https://doi.org/10.1016/j.epsl.2008.04.015, 2008.

Govin, A., Capron, E., Tzedakis, P. C., Verheyden, S., Ghaleb, B., Hillaire-Marcel, C., St-Onge, G., Stoner, J. S., Bassinot, F., Bazin, L., Blunier, T., Combourieu-Nebout, N., El Ouahabi, A., Genty, D., Gersonde, R., Jimenez-Amat, P., Landais, A., Martrat, B., Masson-Delmotte, V., Parrenin, F., Seidenkrantz, M. S., Veres, D., Waelbroeck, C., and Zahn, R.: Sequence of events from the onset to the demise of the Last Interglacial: Evaluating strengths and limitations of chronologies used in

climatic archives, Quat. Sci. Rev., 129, 1–36, https://doi.org/10.1016/j.quascirev.2015.09.018, 2015.

Gray, W. R. and Evans, D.: Nonthermal Influences on Mg/Ca in Planktonic Foraminifera: A Review of Culture Studies and Application to the Last Glacial Maximum, Paleoceanogr. Paleoclimatology, 34, 306–315, https://doi.org/10.1029/2018PA003517, 2019.

Hein, M. and Sand-Jensen, K.: CO2 increases oceanic primary production, Nature, 388, 526–527, https://doi.org/10.1038/41457, 1997.

Henderiks, J.: Coccolithophore size rules - Reconstructing ancient cell geometry and cellular calcite quota from fossil coccoliths, Mar. Micropaleontol., 67, 143–154, https://doi.org/10.1016/j.marmicro.2008.01.005, 2008.

Herbert, T. D.: Alkenone Paleotemperature Determinations, in: Treatise on Geochemistry, vol. 6–9, 391–432, https://doi.org/10.1016/B0-08-043751-6/06115-6, 2003.

Herbert, T. D., Lawrence, K. T., Tzanova, A., Peterson, L. C., Caballero-Gill, R., and Kelly, C. S.: Late Miocene global cooling and the rise of modern ecosystems, Nat. Geosci., 9, 843–847, https://doi.org/10.1038/ngeo2813, 2016.

Hermoso, M.: Coccolith-Derived Isotopic Proxies in Palaeoceanography: Where Geologists Need Biologists, Cryptogam. Algol., 35, 323–351, https://doi.org/10.7872/crya.v35.iss4.2014.323, 2014.

Hermoso, M.: Isotopic record of Pleistocene glacial/interglacial cycles in pelagic carbonates: Revisiting historical data from the Caribbean Sea, Quat. Sci. Rev., 137, 69–78, https://doi.org/10.1016/j.quascirev.2016.02.003, 2016.

Hermoso, M., Candelier, Y., Browning, T. J., and Minoletti, F.: Environmental control of the isotopic composition of subfossil coccolith calcite: Are laboratory culture data transferable to the natural environment?, 7, 35–42, https://doi.org/10.1016/j.grj.2015.05.002, 2015.

Hermoso, M., Minoletti, F., Aloisi, G., Bonifacie, M., McClelland, H. L. O., Labourdette, N., Renforth, P., Chaduteau, C., and Rickaby, R. E. M.: An explanation for the 18O excess in Noelaerhabdaceae coccolith calcite, Geochim. Cosmochim. Acta, 189, 132–142, https://doi.org/10.1016/j.gca.2016.06.016, 2016a.

Hermoso, M., Chan, I. Z. X., McClelland, H. L. O., Heureux, A. M. C., and Rickaby, R. E. M.: Vanishing coccolith vital effects with alleviated carbon limitation, Biogeosciences, 13, 301–312, https://doi.org/10.5194/bg-13-301-2016, 2016b.

Hermoso, M., Godbillot, C., and Minoletti, F.: Enhancing Our Palaeoceanographic Toolbox Using Paired Foraminiferal and Coccolith Calcite Measurements From Pelagic Sequences, Front. Earth Sci., 8, 1–5, https://doi.org/10.3389/feart.2020.00038, 2020a.

Hermoso, M., McClelland, H.-L. O., Hirst, J. S., Minoletti, F., Bonifacie, M., and Rickaby, R. E. M.: Towards the use of the coccolith vital effects in palaeoceanography: A field investigation during the middle Miocene in the SW Pacific Ocean, Deep Sea Res. Part I Oceanogr. Res. Pap., 38, 103262, https://doi.org/10.1016/j.dsr.2020.103262, 2020b.

Huete-Ortega, M., Cermeño, P., Calvo-Díaz, A., and Marañón, E.: Isometric size-scaling of metabolic rate and the size abundance distribution of phytoplankton, Proc. R. Soc. B Biol. Sci., 279, 1815–1823, https://doi.org/10.1098/rspb.2011.2257, 2012.

Jasper, J. P., Hayes, J. M., Mix, A. C., and Prahl, F. G.: Photosynthetic fractionation of 13C and concentrations of dissolved

CO2 in the central equatorial Pacific during the last 255,000 years, Paleoceanography, 9, 781–798, https://doi.org/10.1029/94PA02116, 1994.

Jiménez-Amat, P. and Zahn, R.: Offset timing of climate oscillations during the last two glacial-interglacial transitions connected with large-scale freshwater perturbation, Paleoceanography, 30, 768–788, https://doi.org/10.1002/2014PA002710, 2015.

Jin, X., Liu, C., Zhang, H., Zhou, C., Jiang, X., Wu, Z., and Xu, J.: Evolutionary driven of Gephyrocapsa coccolith isotopic vital effects over the past 400 ka, Earth Planet. Sci. Lett., 503, 236–247, https://doi.org/10.1016/j.epsl.2018.09.010, 2018.

Kahn, M. I. and Williams, D. F.: Oxygen and carbon isotopic composition of living planktonic foraminifera from the northeast Pacific Ocean, Palaeogeogr. Palaeoclimatol. Palaeoecol., 33, 47–69, https://doi.org/10.1016/0031-0182(81)90032-8, 1981.

Kim, S.-T. and O'Neil, J. R.: Equilibrium and nonequilibrium oxygen isotope effects in synthetic carbonates, Geochim. Cosmochim. Acta, 61, 3461–3475, https://doi.org/10.1016/S0016-7037(97)00169-5, 1997.

Lévy, M., Lehahn, Y., André, J. M., Mémery, L., Loisel, H., and Heifetz, E.: Production regimes in the northeast Atlantic: A study based on Sea-viewing Wide Field-of-view Sensor (SeaWiFS) chlorophyll and ocean general circulation model mixed layer depth, J. Geophys. Res. C Ocean., 110, 1–16, https://doi.org/10.1029/2004JC002771, 2005.

Lisiecki, L. E. and Raymo, M. E.: A Pliocene-Pleistocene stack of 57 globally distributed benthic δ 18 O records, Paleoceanography, 20, 1–17, https://doi.org/10.1029/2004PA001071, 2005.

Lisiecki, L. E. and Stern, J. V: Regional and global benthic δ 18 O stacks for the last glacial cycle, Paleoceanography, 31, 1368–1394, https://doi.org/10.1002/2016PA003002, 2016.

Locarnini, R. A., Mishonov, A. V., Antonov, J. I., Boyer, T. P., Garcia, H. E., Baranova, O. K., Zweng, M. M., Paver, C. R., Reagan, J. R., Johnson, D. R., Hamilton, M., and Seidov, D.: World Ocean Atlas 2013, Volume 1: Temperature, edited by: Levitus, S. and Mishonov, A. V., 40 pp., 2013.

Lohbeck, K. T., Riebesell, U., and Reusch, T. B. H.: Adaptive evolution of a key phytoplankton species to ocean acidification, Nat. Geosci., 5, 346–351, https://doi.org/10.1038/ngeo1441, 2012.

Lueker, T. J., Dickson, A. G., and Keeling, C. D.: Ocean pCO2 calculated from dissolved inorganic carbon, alkalinity, and equations for K1 and K2: validation based on laboratory measurements of CO2 in gas and seawater at equilibrium, Mar. Chem., 70, 105–119, https://doi.org/10.1016/S0304-4203(00)00022-0, 2000.

Martínez-Botí, M. A., Marino, G., Foster, G. L., Ziveri, P., Henehan, M. J., Rae, J. W. B., Mortyn, P. G., and Vance, D.: Boron isotope evidence for oceanic carbon dioxide leakage during the last deglaciation, Nature, 518, 219–222, https://doi.org/10.1038/nature14155, 2015.

McClelland, H. L. O., Bruggeman, J., Hermoso, M., and Rickaby, R. E. M.: The origin of carbon isotope vital effects in coccolith calcite, Nat. Commun., 8, 1–16, https://doi.org/10.1038/ncomms14511, 2017.

Minoletti, F., Hermoso, M., and Gressier, V.: Separation of sedimentary micron-sized particles for palaeoceanography and calcareous nannoplankton biogeochemistry, Nat. Protoc., 4, 14–24, https://doi.org/10.1038/nprot.2008.200, 2009.

Monteiro, F. M., Bach, L. T., Brownlee, C., Bown, P., Rickaby, R. E. M., Poulton, A. J., Tyrrell, T., Beaufort, L., Dutkiewicz,

S., Gibbs, S., Gutowska, M. A., Lee, R., Riebesell, U., Young, J., and Ridgwell, A.: Why marine phytoplankton calcify, Sci. Adv., 2, e1501822, https://doi.org/10.1126/sciadv.1501822, 2016.

Naafs, B. D. A., Stein, R., Hefter, J., Khélifi, N., De Schepper, S., and Haug, G. H.: Late Pliocene changes in the North Atlantic Current, Earth Planet. Sci. Lett., 298, 434–442, https://doi.org/10.1016/j.epsl.2010.08.023, 2010.

Neftel, A., Oeschger, H., Schwander, J., Stauffer, B., and Zumbrunn, R.: Ice core sample measurements give atmospheric CO2 content during the past 40,000 yr, Nature, 295, 220–223, https://doi.org/10.1038/295220a0, 1982.

Nimer, N., Brownlee, C., and Merrett, M.: Carbon dioxide availability, intracellular pH and growth rate of the coccolithophore Emiliania huxleyi, Mar. Ecol. Prog. Ser., 109, 257–262, https://doi.org/10.3354/meps109257, 1994.

Nimer, N. A., Iglesias-Rodriguez, M. D., and Merrett, M. J.: Bicarbonate utilization by marine phytoplankton species, J. Phycol., 33, 625–631, https://doi.org/10.1111/j.0022-3646.1997.00625.x, 1997.

Omta, A. W., Van Voorn, G. A. K., Rickaby, R. E. M., and Follows, M. J.: On the potential role of marine calcifiers in glacial-interglacial dynamics, Global Biogeochem. Cycles, 27, 692–704, https://doi.org/10.1002/gbc.20060, 2013.

Pagani, M.: Biomarker-Based Inferences of Past Climate: The Alkenone pCO2 Proxy, 2nd ed., Elsevier Ltd., 361-378 pp., https://doi.org/10.1016/B978-0-08-095975-7.01027-5, 2013.

Paillard, D., Labeyrie, L., and Yiou, P.: Macintosh Program performs time-series analysis, Eos, Trans. Am. Geophys. Union, 77, 379–379, https://doi.org/10.1029/96EO00259, 1996.

Pearson, P. N.: Oxygen isotopes in foraminifera: Overview and historical review, Paleontol. Soc. Pap., 18, 1–38, https://doi.org/10.1017/S1089332600002539, 2012.

Petit, J. R., Jouzel, J., Raynaud, D., Barkov, N. I., Barnola, J.-M., Basile, I., Bender, M., Chappellaz, J., Davis, M., Delaygue, G., Delmotte, M., Kotlyakov, V. M., Legrand, M., Lipenkov, V. Y., Lorius, C., PÉpin, L., Ritz, C., Saltzman, E., and Stievenard, M.: Climate and atmospheric history of the past 420,000 years from the Vostok ice core, Antarctica, Nature, 399, 429–436, https://doi.org/10.1038/20859, 1999.

Pflaumann, U., Sarnthein, M., Chapman, M., D'Abreu, L., Funnell, B., Huels, M., Kiefer, T., Maslin, M., Schulz, H., Swallow, J., van Kreveld, S., Vautravers, M., Vogelsang, E., and Weinelt, M.: Glacial North Atlantic: Sea-surface conditions reconstructed by GLAMAP 2000, Paleoceanography, 18, https://doi.org/10.1029/2002PA000774, 2003.

Popp, B. N., Laws, E. A., Bidigare, R. R., Dore, J. E., Hanson, K. L., and Wakeham, S. G.: Effect of phytoplankton cell geometry on carbon isotopic fractionation, Geochim. Cosmochim. Acta, 62, 69–77, https://doi.org/10.1016/S0016-7037(97)00333-5, 1998.

Rae, J. W. B., Zhang, Y. G., Liu, X., Foster, G. L., Stoll, H. M., and Whiteford, R. D. M.: Atmospheric CO 2 over the Past 66 Million Years from Marine Archives, Annu. Rev. Earth Planet. Sci., 49, 609–641, https://doi.org/10.1146/annurev-earth-082420-063026, 2021.

Rebotim, A., Voelker, A. H. L., Jonkers, L., Waniek, J. J., Meggers, H., Schiebel, R., Fraile, I., Schulz, M., and Kucera, M.: Factors controlling the depth habitat of planktonic foraminifera in the subtropical eastern North Atlantic, Biogeosciences, 14, 827–859, https://doi.org/10.5194/bg-14-827-2017, 2017.

Reinfelder, J. R.: Carbon Concentrating Mechanisms in Eukaryotic Marine Phytoplankton, Ann. Rev. Mar. Sci., 3, 291–315, https://doi.org/10.1146/annurev-marine-120709-142720, 2011.

Rickaby, R. E. M., Henderiks, J., and Young, J. N.: Perturbing phytoplankton: Response and isotopic fractionation with changing carbonate chemistry in two coccolithophore species, Clim. Past, 6, 771–785, https://doi.org/10.5194/cp-6-771-2010, 2010.

Sanyal, A., Hemming, N. G., Hanson, G. N., and Broecker, W. S.: Evidence for a higher pH in the glacial ocean from boron isotopes in foraminifera, Nature, 373, 234–236, https://doi.org/10.1038/373234a0, 1995.

Shao, J., Stott, L. D., Gray, W. R., Greenop, R., Pecher, I., Neil, H. L., Coffin, R. B., Davy, B., and Rae, J. W. B.: Atmosphere-Ocean CO2 Exchange Across the Last Deglaciation From the Boron Isotope Proxy, Paleoceanogr. Paleoclimatology, 34, 1650–1670, https://doi.org/10.1029/2018PA003498, 2019.

Skinner, L. C., Fallon, S., Waelbroeck, C., Michel, E., and Barker, S.: Ventilation of the Deep Southern Ocean and Deglacial CO2 Rise, Science (80-.)., 328, 1147–1151, https://doi.org/10.1126/science.1183627, 2010.

Skinner, L. C., Primeau, F., Freeman, E., De La Fuente, M., Goodwin, P. A., Gottschalk, J., Huang, E., McCave, I. N., Noble, T. L., and Scrivner, A. E.: Radiocarbon constraints on the glacial ocean circulation and its impact on atmospheric CO2, Nat. Commun., 8, 1–10, https://doi.org/10.1038/ncomms16010, 2017.

Spratt, R. M. and Lisiecki, L. E.: A Late Pleistocene sea level stack, Clim. Past, 12, 1079–1092, https://doi.org/10.5194/cp-12-1079-2016, 2016.

Stein, R., Hefter, J., Grützner, J., Voelker, A., and Naafs, B. D. A.: Variability of surface water characteristics and Heinrich-like events in the Pleistocene midlatitude North Atlantic Ocean: Biomarker and XRD records from IODP Site U1313 (MIS 16-9), Paleoceanography, 24, n/a-n/a, https://doi.org/10.1029/2008PA001639, 2009.

Stoll, H. M., Guitian, J., Hernandez, I., Mejia, L. M., Phelps, S., Rosenthal, Y., Zhang, H., and Ziveri, P.: Upregulation of phytoplankton carbon concentrating mechanisms during low CO2 glacial periods and implications for the phytoplankton pCO2 proxy, Quat. Sci. Rev., 208, 1–20, https://doi.org/10.1016/j.quascirev.2019.01.012, 2019.

Takahashi, T., Sutherland, S. C., and Kozyr, A.: Global Ocean Surface Water Partial Pressure of CO2 Database: Measurements Performed During 1957–2010 (Version 2010), ORNL/CDIAC-159, NDP-088(V2010). Carbon Dioxide Information Analysis Center, Oak Ridge National Laboratory, U.S. Department of Energy, Oak Ridge, Tennessee, https://doi.org/10.3334/CDIAC/otg.ndp088(V2010), 2011.

Tremblin, M., Hermoso, M., and Minoletti, F.: Equatorial heat accumulation as a long-term trigger of permanent Antarctic ice sheets during the Cenozoic, Proc. Natl. Acad. Sci., 113, 11782–11787, https://doi.org/10.1073/pnas.1608100113, 2016.

Tzedakis, P. C., Drysdale, R. N., Margari, V., Skinner, L. C., Menviel, L., Rhodes, R. H., Taschetto, A. S., Hodell, D. A., Crowhurst, S. J., Hellstrom, J. C., Fallick, A. E., Grimalt, J. O., McManus, J. F., Martrat, B., Mokeddem, Z., Parrenin, F., Regattieri, E., Roe, K., and Zanchetta, G.: Enhanced climate instability in the North Atlantic and southern Europe during the Last Interglacial, Nat. Commun., 9, https://doi.org/10.1038/s41467-018-06683-3, 2018.

de Vargas, C., Aubry, M. P., Probert, I., and Young, J.: Origin and Evolution of Coccolithophores. From Coastal Hunters to

Oceanic Farmers., Evol. Prim. Prod. Sea, 251–285, https://doi.org/10.1016/B978-012370518-1/50013-8, 2007.

De Vernal, A., Eynaud, F., Henry, M., Hillaire-Marcel, C., Londeix, L., Mangin, S., Matthiessen, J., Marret, F., Radi, T., Rochon, A., Solignac, S., and Turon, J. L.: Reconstruction of sea-surface conditions at middle to high latitudes of the Northern Hemisphere during the Last Glacial Maximum (LGM) based on dinoflagellate cyst assemblages, Quat. Sci. Rev., 24, 897–924, https://doi.org/10.1016/j.quascirev.2004.06.014, 2005.

Villanueva, J., Grimalt, J. O., Cortijo, E., Vidal, L., and Labeyrie, L.: Assessment of sea surface temperature variations in the central North Atlantic using the alkenone unsaturation index (U37(k')), Geochim. Cosmochim. Acta, 62, 2421–2427, https://doi.org/10.1016/S0016-7037(98)00180-X, 1998.

Villanueva, J., Calvo, E., Pelejero, C., Grimalt, J. O., Boelaert, A., and Labeyrie, L.: A latitudinal productivity band in the Central North Atlantic over the last 270 kyr: An alkelone perspective, Paleoceanography, 16, 617–626, https://doi.org/10.1029/2000PA000543, 2001.

Volkman, J. K., Eglinton, G., Corner, E. D. S., and Sargent, J. R.: Novel unsaturated straight-chain C37-C39 methyl and ethyl ketones in marine sediments and a coccolithophore Emiliania huxleyi, Phys. Chem. Earth, 12, 219–227, https://doi.org/10.1016/0079-1946(79)90106-X, 1980.

Winter, A., Rost, B., Hilbrecht, H., and Elbrächter, M.: Vertical and horizontal distribution of coccolithophores in the Caribbean Sea, Geo-Marine Lett., 22, 150–161, https://doi.org/10.1007/s00367-002-0108-8, 2002.

Zeebe, R. E. and Wolf-Gladrow, D.: CO2 in seawater: equilibrium, kinetics, isotopes, Elsevier O., Elsevier Science, 360 pp., 2001.

Zhang, X., Knorr, G., Lohmann, G., and Barker, S.: Abrupt North Atlantic circulation changes in response to gradual CO 2 forcing in a glacial climate state, Nat. Geosci., 10, 518–523, https://doi.org/10.1038/ngeo2974, 2017.

Zhang, Y. G., Pagani, M., Liu, Z., Bohaty, S. M., and DeConto, R.: A 40-million-year history of atmospheric CO 2, Philos. Trans. R. Soc. A Math. Phys. Eng. Sci., 371, 20130096, https://doi.org/10.1098/rsta.2013.0096, 2013.

Ziveri, P., Stoll, H., Probert, I., Klaas, C., Geisen, M., Ganssen, G., and Young, J.: Stable isotope "vital effects" in coccolith calcite, Earth Planet. Sci. Lett., 210, 137–149, https://doi.org/10.1016/S0012-821X(03)00101-8, 2003.

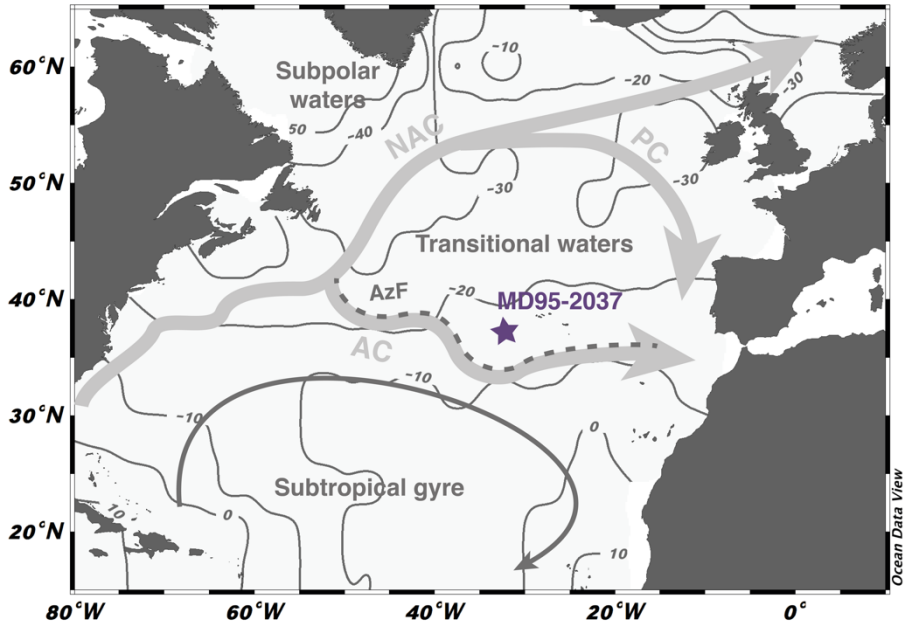

Figure 1: Location and hydrological settings of core MD95-2037. The core lies north of the Azores Current (AC) and the associated Azores Front (AzF), a branch of the North Atlantic Current (NAC). It is located in the transitional waters delimited to the north by the Portugal Current (PC). Site location overlays a map of mean annual ΔpCO_2 (in ppm, Takahashi et al 2011) compiled with the Ocean Data View software (Schlitzer, 2018, http://odv.awi.de). Regions with positive (negative) values are sources (sinks) for atmospheric CO_2.

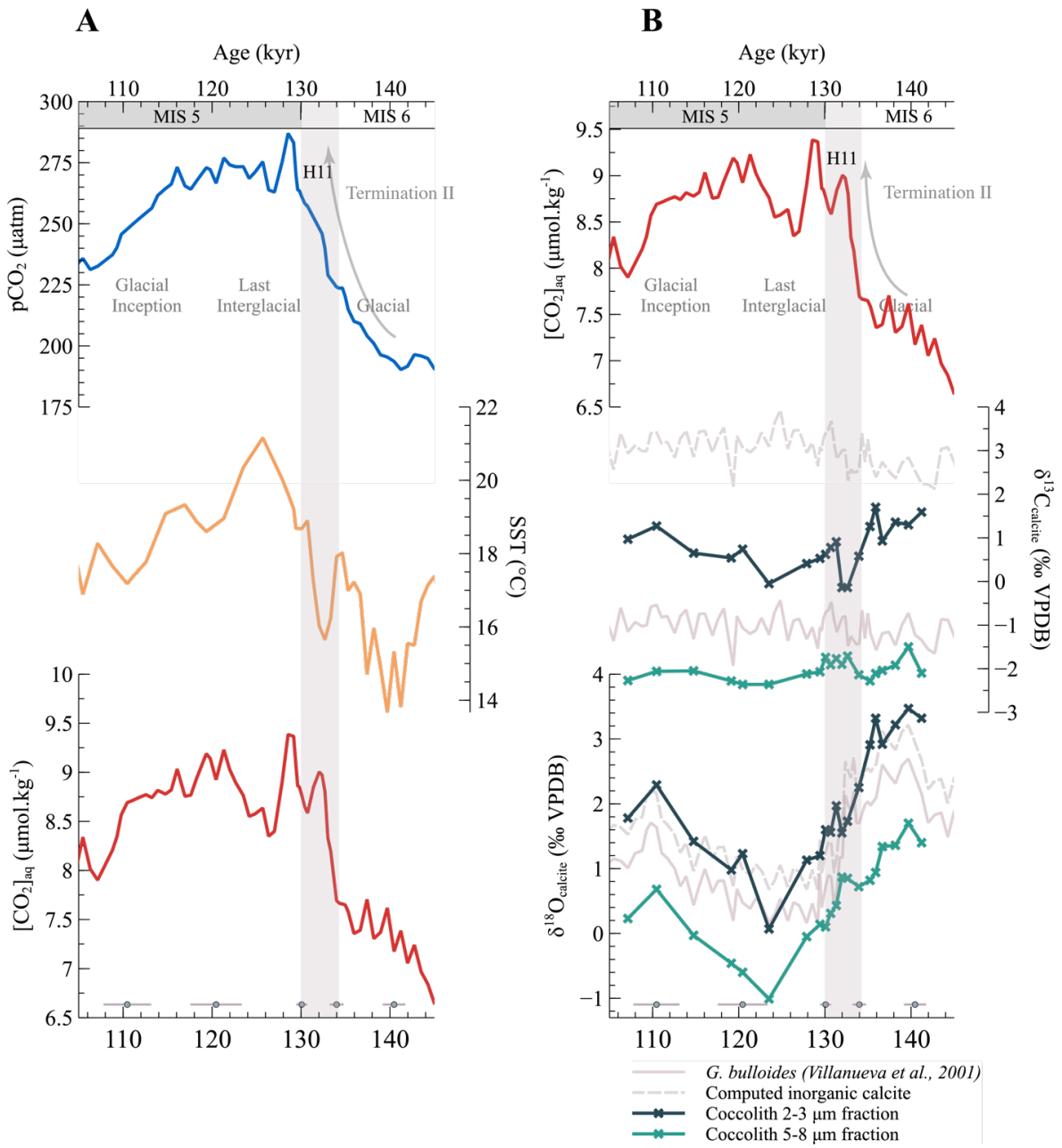

Figure 2: Deglacial changes in the isotopic composition of coccolith size fractions, sea surface temperatures and aqueous CO_2 concentrations. Panel A: the aqueous CO_2 curve is derived from the ice core pCO_2 (Bereiter et al., 2015) and sea surface temperature (SST) records from Calvo et al., 2001 (see Methods section). Panel B: changes in coccolith $\delta^{13}C$ and $\delta^{18}O$ per size fraction considered across the interval. Also reported are the values of the isotopic composition of foraminifera *G. bulloides* calcite (Villanueva et al, 2001) from which we tentatively derived values for the $\delta^{13}C$ and $\delta^{18}O$ of inorganic calcite (see Methods section). Age uncertainties over the interval of study are shown (bottom grey points).

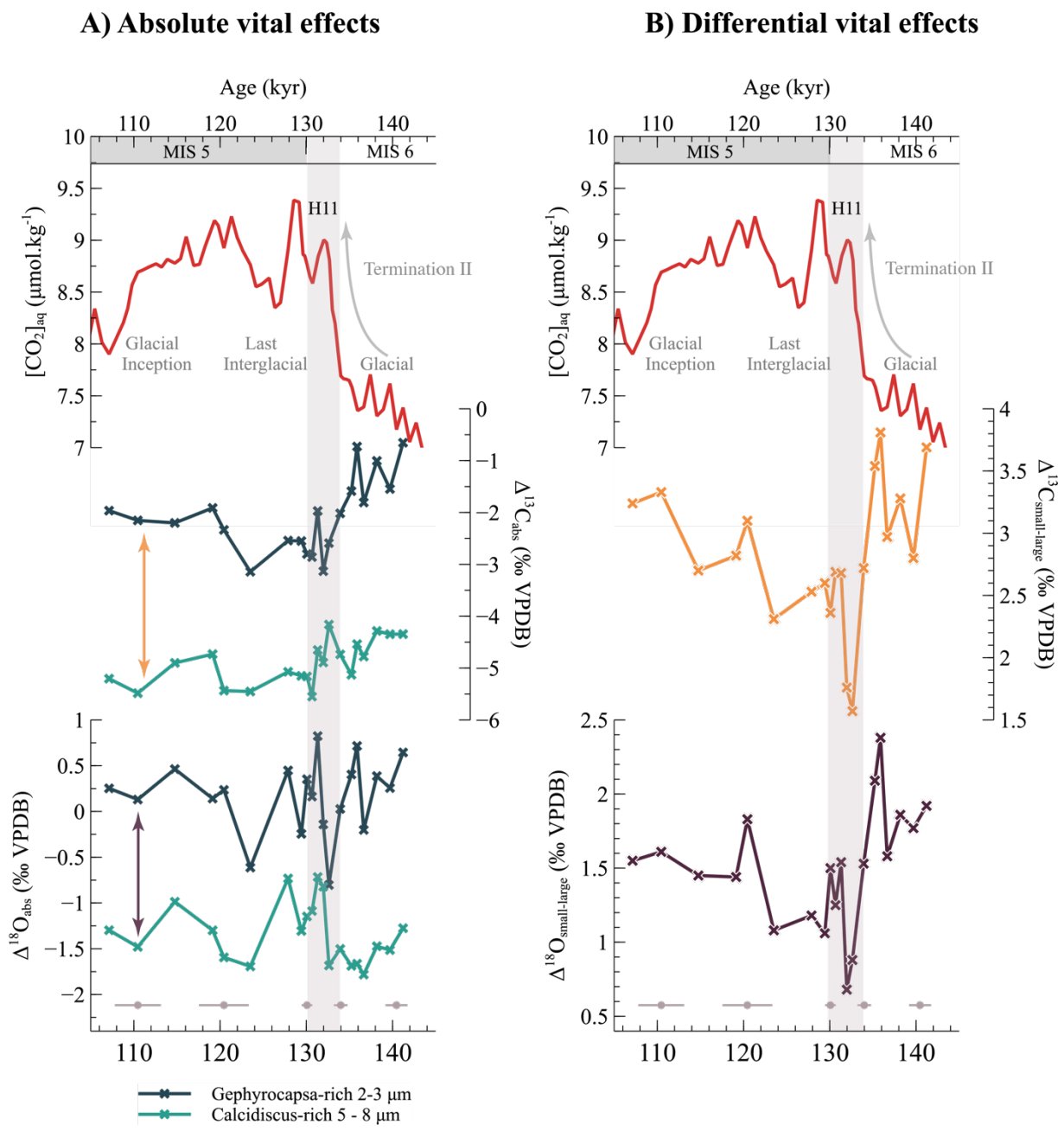

Figure 3: Expression of the coccolith vital effects, both absolute (A) and differential (B), across Termination II. A: the magnitude of the coccolith absolute vital effect seems to be dependent on coccolith size. Arrows in panel A represent the differential vital effects represented in the associated panel B: the differential vital effect in both carbon and oxygen isotopes is less marked during the interglacial with high aqueous CO_2 concentrations than during the glacial maximum.

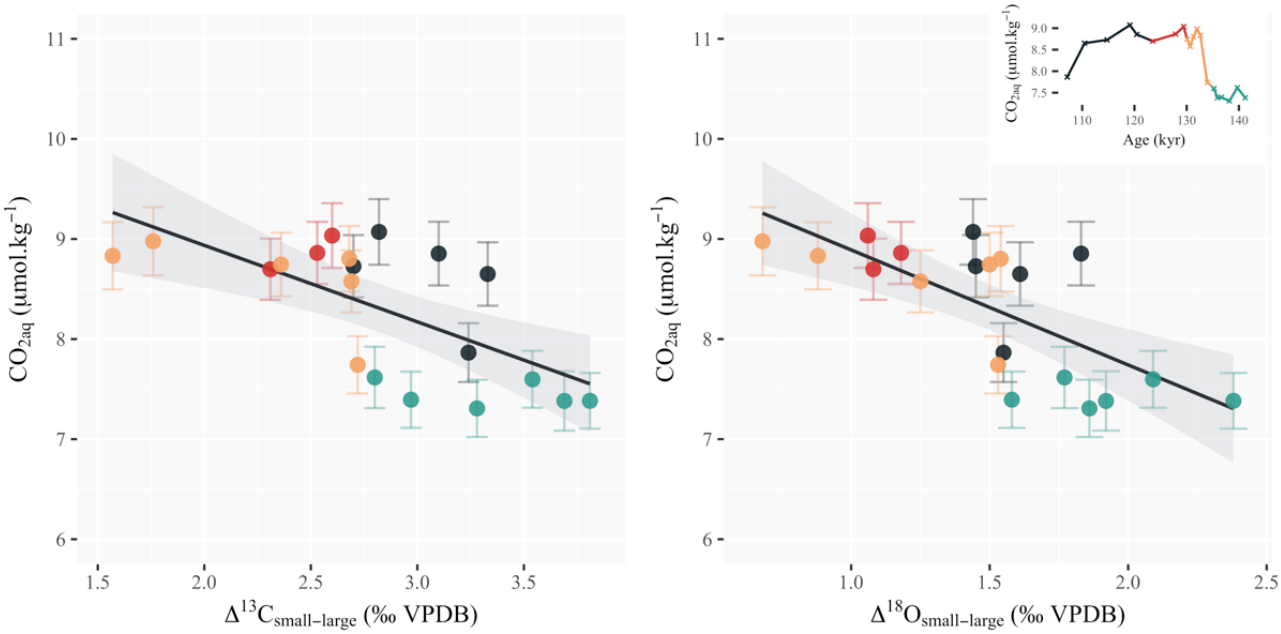

Figure 4: Scatter plots of the differential vital effects in carbon and oxygen vs. aqueous CO_2 concentration. $\Delta^{13}C_{small-large}$ and $\Delta^{18}O_{small-large}$ correlate with changes in the ambient CO_2 concentrations (R^2 =0.44, $p < 10^{-2}$ and R^2 = 0.51, $p < 10^{-3}$ respectively). Data points are colored according to the time period considered: the glacial maximum (green), Heinrich Event 11 (orange), the interglacial (red) and glacial inception (black). Inset are the surface ocean CO_2 concentrations across the deglaciation (calculations are detailed in the Material and Methods section).

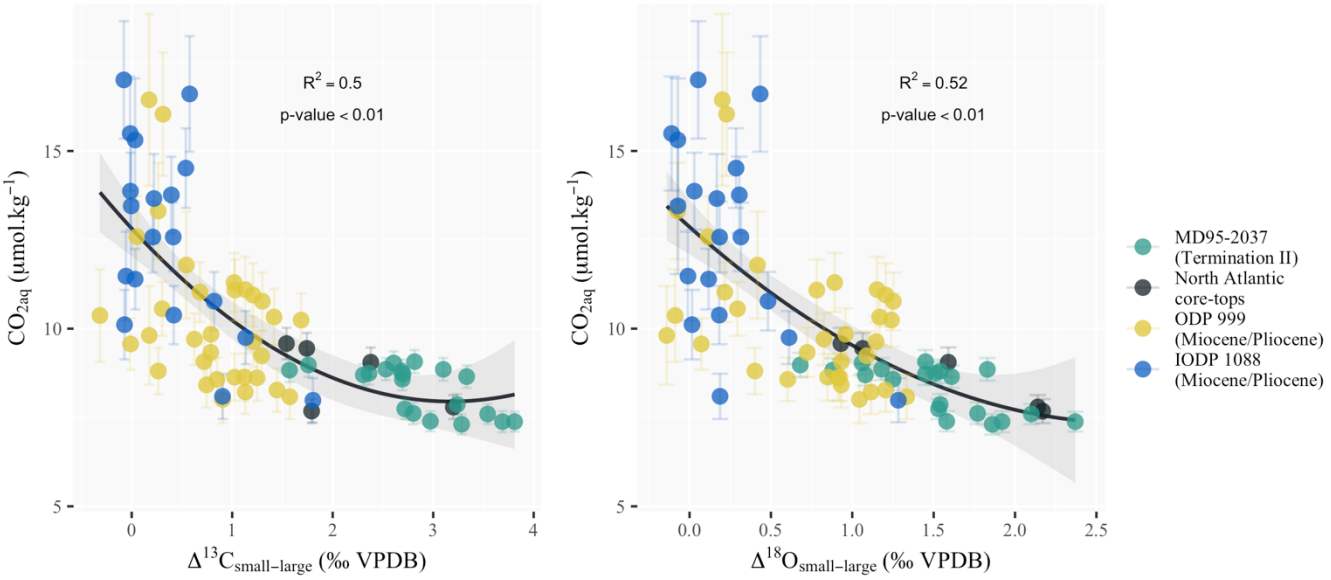

Figure 5: Coccolith differential vital effect sensitivity to changes in aqueous CO_2 since the Miocene. Differential vital effects are more important in the Late Pleistocene and modern-day ocean than during the Miocene. The correlation between aqueous CO_2 and differential vital effects in carbon ($R^2 = 0.5$) or oxygen ($R^2 = 0.52$) suggests that an increase in carbon limitation might be responsible for the observed change. Coccolith vital effect datasets are from (Bolton et al., 2012) for the Miocene and Pliocene, and Candelier et al. 2013 and Hermoso et al. 2015 for the North Atlantic core-tops. The pCO_2 records used to compute aqueous CO_2 for the Miocene and Pliocene datasets are from Rae et al., 2021. SST data for site 1088 are from Herbert et al. 2016. For site 999 we took the composite SST record from Rae et al., 2021, as no SST dataset spanned the whole of the differential vital effect record for site 999. Core-top CO_2 concentrations were calculated using a pre-industrial pCO_2 of 280 ppm and SST data from WOA13 (Locarnini et al., 2013) .